ELSEVIER

Surface Science 502–503 (2002) 109–122

SURFACE SCIENCE

www.elsevier.com/locate/susc

Sum frequency generation vibrational spectroscopy at solid–gas interfaces: CO adsorption on Pd model catalysts at ambient pressure

Günther Rupprechter *, Holger Unterhalt, Matthias Morkel, Paolo Galletto, Linjie Hu, Hans-Joachim Freund

Fritz-Haber-Institut der Max-Planck-Gesellschaft, Department of Chemical Physics, Faradayweg 4-6, D-14195 Berlin, Germany

Abstract

Carbon monoxide adsorption on Pd(1 1 1) and Pd nanoparticles supported by Al_2O_3/NiAl(1 1 0) was examined by vibrational sum frequency generation spectroscopy from 10^{-8} to 1000 mbar, and from 100 to 400 K. Identical CO saturation structures were observed on Pd(1 1 1) under ultrahigh vacuum ($\sim 10^{-7}$ mbar, 95 K) and at high pressure (e.g. $\geqslant 1$ mbar, 190 K) with no indications of pressure-induced surface rearrangements. Special attention was paid to experimental artifacts that may occur under elevated pressure and may be misinterpreted as "high pressure effects". Vibrational spectra of CO on defect-rich Pd(1 1 1) exhibited an additional peak that originated from CO bound to defect (step or edge) sites. The CO adsorbate structure on supported Pd nanoparticles was different from Pd(1 1 1) but more similar to stepped Pd(1 1 1). At low pressure (10^{-7} mbar CO) the adsorbate structure depended strongly on the Pd morphology revealing specific differences in the adsorption properties of supported nanoparticles and single crystal surfaces. At high pressure (e.g. 200 mbar CO) these differences were even more pronounced. Prominent high coverage CO structures on Pd(1 1 1) could not be established on Pd particles. However, in spite of structural differences between well faceted and rough Pd nanoparticles nearly identical adsorption site occupancies were observed in both cases at 200 mbar CO. Initial tests of the catalytic activity of Pd/Al_2O_3/NiAl(1 1 0) for ethylene hydrogenation at 1 bar revealed a remarkable activity and stability of the model system with catalytic properties similar to impregnated catalysts.

Keywords: Sum frequency generation; Catalysis; Vibrations of adsorbed molecules; Palladium; Carbon monoxide; Low index single crystal surfaces; Clusters

1. Introduction

The relevance of studies of surface processes under ultrahigh vacuum (UHV) for technical catalysis has been under debate for long, with controversial evidence in favor and against it [1,2]. It has been speculated that in some cases active species may only appear at high pressure ($\geqslant 1$ mbar) while being absent under UHV. There are several scenarios that can account for such an effect. High pressures may be able to produce surface coverages exceeding the UHV saturation coverage thereby producing new adsorbate

* Corresponding author. Fax: +49-30-8413-4105.
E-mail address: rupprechter@fhi-berlin.mpg.de (G. Rupprechter).

0039-6028/02/$ - see front matter
PII: S0039-6028(01)01907-0

structures (e.g. observed for CO on Pt(1 1 1) by STM [3]). Of course, high coverages can also be obtained under UHV but generally only at low temperature (e.g. 100 K). However, at low temperature a catalytic reaction may proceed in a different way and, furthermore, the reduced mobility of the adsorbed molecules may influence the adsorbate structure. Another scenario involves weakly bound active species that only occur close to saturation coverage after all stronger bonding sites are already occupied by spectator species [4]. At elevated temperature higher pressures than those usually applied in UHV studies ($\sim 10^{-6}$ mbar) may be required to produce that coverage regime that is relevant for a reaction. Up to now we have implied that the surface under investigation would remain "rigid". However, it has been reported that catalysts may restructure at elevated pressure and temperature, e.g. when volatile or mobile components such as carbonyls are involved [5–8]. It is clear that this has an impact on the available adsorption sites and thus on the adsorbate structure. The surface composition may also depend on pressure, for instance by changing from oxygen adsorbed on a metal surface to a surface metal oxide [9] or to a metastable suboxide that cannot be identified in UHV or by ex situ analysis [10]. In the latter two situations UHV and high pressure studies would simply examine different materials, the occurrence of discrepancies is therefore "apparent" (of course, only after one has understood the involved processes!). A clear-cut separation of these effects is not possible and their occurrence depends on the material under investigation. A general answer to these questions is therefore still at large but the interest to narrow the gap between catalysis and surface science has stimulated the development of surface-sensitive techniques which can operate under technically relevant conditions (for an overview see Refs. [1,2,4]). This has promoted photon based techniques such as sum frequency generation (SFG) which are not restricted to a vacuum environment.

As a second order non-linear optical process, infrared-visible SFG is forbidden in media with inversion symmetry under the electric dipole approximation, but allowed at the surface/interface where the inversion symmetry is broken [11]. Consequently, SFG specifically probes the interfacial region between two isotropic media providing information on molecular interaction and orientation. In its spectroscopic application using a frequency-tunable IR beam, vibrational SFG spectroscopy has been employed to study solid–gas interaction [4,12], but also buried interfaces such as solid–liquid and liquid–liquid were examined [11,13,14]. With respect to catalysis the major benefit of SFG is its ability to provide vibrational spectra of adsorbates from submonolayer quantities in UHV up to ambient gas pressure (the adsorbate representing the interface between the isotropic gas phase and a centrosymmetric metal surface).

First SFG studies were carried out on single crystal surfaces such as Ni(1 0 0) [12], Pt(1 1 1) and Pt(1 1 0) [15–17] since these "mirror-like" surfaces facilitated the optical experiment. Later on, less-ideal substrates like thin oxide films [18] and polycrystalline foil [19] were examined and, finally, the material range was extended to metal nanoparticles supported on a thin oxide film [20,21]. Most attention was directed to the adsorption of CO, NO and small hydrocarbons. Summarizing, SFG spectroscopy can be applied to a variety of model surfaces and can also cover the pressure range from UHV to atmospheric pressure. It is clear that SFG is a promising route to interconnect surface science and technical catalysis.

In this paper, SFG is employed to examine CO adsorption over a wide range of pressure/temperature (10^{-8} to 1000 mbar, 100 to 400 K) in order to identify high pressure effects. To cover different kinds of model surfaces, experiments were carried out on Pd(1 1 1), on "defect-rich" Pd(1 1 1) and on alumina supported Pd nanoparticles utilizing a UHV surface analysis system combined with an SFG-compatible UHV/high pressure cell. Part of the results were presented in separate preceding publications, here we will try to obtain a broader view and contrast our results to previous (UHV) IRAS studies on single crystals [22–25] and nanoparticles [26–28]. We will also discuss experimental artifacts that may occur under elevated pressure and may be misinterpreted as "high pressure effects". In order to test how well UHV-grown $Pd/Al_2O_3/NiAl(1\,1\,0)$ model catalysts can

mimic a technical (impregnated) catalyst, their catalytic activity for ethylene hydrogenation at 1 bar was determined and compared to powder catalysts.

2. Experimental

In order to combine SFG with well-established surface characterization methods such as low energy electron diffraction (LEED), Auger electron spectroscopy (AES) and temperature programmed desorption (TPD) we have built an instrument that allows us to prepare and characterize model catalysts in UHV, transfer the samples into a high pressure cell, and to monitor adsorbates by SFG spectroscopy. Our two-level chamber design and the SFG process have been described in previous publications and we will only discuss a few aspects here [29,30].

Model catalysts were prepared in the UHV level (base pressure 1×10^{-10} mbar). The sample crystal was spotwelded to two Mo rods and could be resistively heated to 1300 K, and cooled with liquid N_2 to 85 K. After preparation the samples were transferred under UHV into the SFG-compatible UHV-high pressure cell equipped with CaF_2 windows. During this operation the sample holder was introduced into three differentially pumped spring-loaded teflon seals separating the UHV and high pressure sections. The reaction cell could be pressurized to 1 bar while keeping the preparation chamber at 5×10^{-10} mbar. Low exposures were applied using a leak valve and an ionization gauge. For catalytic tests the SFG cell served as recirculated batch reactor interfaced to a gas chromatograph for product analysis. To avoid/minimize wall reactions the SFG-cell was gold coated.

Pd(1 1 1) surfaces were prepared by cutting and polishing, followed by sequences of Ar ion bombardment (beam energy 700 eV at 3×10^{-4} mbar Ar), annealing to 1200 K and oxidation between 1200 and 600 K in 5×10^{-7} mbar O_2, followed by a final flash to 1200 K. The surface structure and cleanliness were examined by LEED, AES, and TPD (results presented elsewhere [31]). Defect-rich Pd(1 1 1) surfaces, i.e. slightly misoriented Pd(1 1 1) or strongly sputtered surfaces (700 eV Ar at 100 K, without subsequent annealing) were also studied. AES indicated that these surfaces were clean, but LEED showed a 1×1 pattern with rather broad spots.

Details about the preparation and characterization of Pd nanoparticles supported on Al_2O_3 can be found in Ref. [32]. An ordered aluminum oxide film was grown by oxidizing a NiAl(1 1 0) substrate in 10^{-5} mbar oxygen at 523 K. Then, Pd was deposited by electron beam evaporation. The mean Pd particle size and (surface) structure were adjusted by controlling the substrate temperature during deposition and the amount of deposited metal. Particles of 3.5 nm mean size (or 850 atoms/particle; particle density 4.5×10^{12} cm^{-2}) were grown on Al_2O_3 at 90 K by depositing a nominal Pd thickness of 0.6 nm, whereas 6 nm particles (or 4000 atoms/particle; particle density 1×10^{12} cm^{-2}) were formed by depositing the same Pd amount at 300 K.

SFG spectrometers based on different lasers have been repeatedly described in the literature [4,11,12,18,19,33–36]. Briefly, to acquire an SFG vibrational spectrum of adsorbate molecules on a catalyst surface, laser pulses at a tunable infrared frequency ω_{IR} and at a fixed visible frequency ω_{VIS} are spatially and temporally overlapped on the sample. When the IR frequency is scanned over a vibrational resonance of the adsorbate, an SFG signal is generated at the sum frequency ($\omega_{SFG} = \omega_{IR} + \omega_{vis}$), i.e. in the visible region. Plotting the SFG intensity as a function of the IR frequency (wavenumber) thus results in the vibrational spectrum. The intensity of the SFG signal is proportional to the absolute square of the second order surface susceptibility $\chi_s^{(2)}$ and to the intensities I_{IR} and I_{vis} of the incoming IR and vis pulses (Eq. (1)).

$$I_{SFG} \propto |\chi_s^{(2)}|^2 I_{IR} I_{vis} \quad (1)$$

Since SFG is not allowed in media with inversion symmetry ($\chi^{(2)} = 0$ in the electric dipole approximation) the process can sensitively probe regions of broken inversion symmetry in otherwise centrosymmetric media, e.g. the boundary between an isotropic gas phase and a centrosymmetric crystal. In the present case, the SFG signal is mainly generated by adsorbed CO, while the

centrosymmetric Pd bulk and the isotropic gas phase give only a small contribution to the signal. It is apparent from Eq. (1) that the SFG signal must be normalized to the IR and vis intensities in the experiment, unless they are constant. This point is particularly important in the presence of a gas phase, as will be discussed below.

The surface susceptibility $\chi_s^{(2)}$ has resonant contributions from the adsorbate vibrations $\chi_R^{(2)}$ (containing the resonance condition $(\omega_{IR} - \omega_q)$), and a non-resonant contribution from the surface itself $\chi_{NR}^{(2)}$. The non-resonant response is often modeled by a frequency independent non-resonant susceptibility $\chi_{NR}^{(2)}$ since the applied light frequencies are far from resonances of the surface.

$$\chi_s^{(2)} = \chi_R^{(2)} + \chi_{NR}^{(2)} = \sum_q \frac{A_{R(q)}}{\omega_{IR} - \omega_q + i\Gamma_q} + A_{NR} e^{i\Phi} \quad (2)$$

$A_{R(q)}$, ω_q, Γ_q and ω_{IR}, refer to the amplitude, resonance frequency and damping constant (homogeneous linewidth $2\Gamma_q = \text{FWHM}$) of the qth vibrationally resonant mode, and to the infrared laser frequency, respectively. $A_{R(q)}$ is proportional to the adsorbate concentration N and to the infrared and Raman transition moments of the vibration. Consequently, a vibration must have non-vanishing infrared and Raman transition moments in order to be SFG active. A_{NR} is the amplitude of the vibrationally non-resonant susceptibility and Φ is its phase relative to the resonant term. Depending on the amplitude and relative phase of both contributions the line shape of the measured SFG signal can vary [33,35,37] but in the present experiments the resonant SFG signal is often much higher than the non-resonant background, producing Lorentzian-like line shapes.

Two different laser systems were employed. SFG on Pd(1 1 1) was performed using a Nd:YAG laser (1064 nm, 30 mJ/pulse, 20 ps, 50 Hz) with part of the output converted to 532 nm and 355 nm by a harmonic generator (SHG, THG) unit. About 200 μJ/pulse 532 nm light was used as visible input, the 1064 nm and 355 nm beams were mixed in a optical parametric generator (OPG)/difference frequency generator (DFG) system to generate tunable infrared light (3–6 μm, ≈150 μJ/pulse, resolution ∼5 cm^{-1}). SFG spectroscopy on Pd particles was performed using an amplified titanium sapphire laser (790 nm, 2 mJ/pulse, 2 ps, 500 Hz) with 90% of its output used to generate tunable infrared light at an approximately constant power between 2000 and 3300 cm^{-1} (∼10 μJ/pulse; 25 cm^{-1} resolution). Below 1900 cm^{-1}, the infrared power decreased significantly preventing SFG investigations in this spectral region. In both configurations, the visible and infrared beams were parallel polarized and at an angle of about 50°. The output SFG beam was left unpolarized, passed to an edge filter and monochromator, and detected via a photomultiplier/boxcar integrator. The IR frequency was calibrated to ±3 cm^{-1} by measurements of the absorption bands of CO at high pressure and of atmospheric CO_2.

3. Results and discussion

3.1. Adsorption of CO on Pd(1 1 1) and defect-rich Pd(1 1 1)

CO on Pd(1 1 1) has received much attention and many IRAS, LEED and TPD studies were reported, e.g. by Bradshaw and coworkers [22], Hoffmann [23], Ertl and coworkers [38], Somorjai and coworkers [39], Goodman and coworkers [24] and others. A variety of ordered CO structures has been reported, e.g. a $(\sqrt{3} \times \sqrt{3})$R30° at 0.33 ML, a c(4 × 2) at 0.5 ML, a $(4\sqrt{3} \times 8)$rect at 0.63 ML and a (2 × 2) at 0.75 ML (1 ML equals the density of Pd atoms in the (1 1 1) plane; 1.53×10^{15} cm^{-2}). IRAS spectra up to 10 mbar CO by Goodman and coworkers [24,40] allowed to construct a so-called "phase diagram" of equilibrium CO structures.

The SFG spectra in Fig. 1 show that the vibrational spectrum of CO on Pd(1 1 1) strongly depends on coverage, in agreement with IRAS [22–24]. Coverages were obtained from TPD [31] and from comparisons with previous IRAS/TPD studies. CO initially adsorbed in threefold hollow sites with stretching frequencies from 1830 to 1900 cm^{-1}. At half monolayer coverage a peak at 1925 cm^{-1} was observed that is attributed to CO in fcc and hcp threefold hollow sites, according to recent photoemission and photoelectron diffrac-

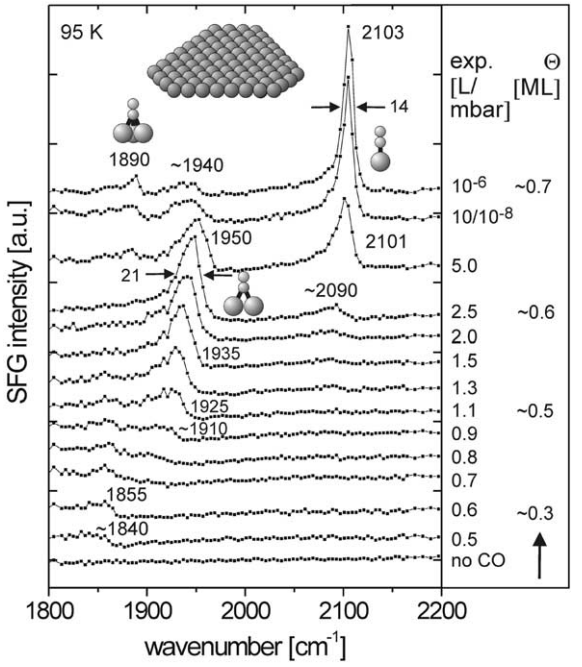

Fig. 1. SFG spectra acquired at increasing CO exposure of Pd(1 1 1) at 95 K. Approximate coverages are also indicated (see text).

tion studies [41,42] and stretching frequency calculations [43]. Around $\theta = 0.6$, CO is preferentially bridge bonded (1950 cm^{-1}) with a smaller amount of linear (on-top) CO (~2090 cm^{-1}). If the coverage is further increased, the bridge site intensity decreased, the on-top signal increased and a transition [24] from a bridge/on-top structure to a hollow/on-top structure occurred. Finally, at saturation coverage (2×2, $\theta = 0.75$) two bands at 1890 and 2103 cm^{-1} (hollow and on-top CO) were observed (the small feature at 1940 cm^{-1} will be discussed below).

Although the SFG spectra in Fig. 1 qualitatively agree with IRAS data [22–24], differences can be recognized that are due to the different selection rules of SFG and IRAS. When Fig. 1 is compared with corresponding spectra in Refs. [22–24] it is evident that SFG "underestimates" multiple-coordinated CO thus leading to a dominant on-top peak. In particular, the hollow peak at 1890 cm^{-1} is too small and the same is true for bridge bonded CO (a similar effect occurred for CO/Pt(1 1 1) [15,17,30]). Since the SFG intensity depends on both the infrared and Raman transition moments the lower sensitivity of SFG towards hollow and bridged species is presumably related to the low Raman polarizability of multiple-coordinated CO or may originate from an interference effect between different SFG susceptibility tensor elements as shown by Baldelli et al. [44]. A quantitative coverage analysis from the peak areas/heights is difficult but the strong coverage-dependence of the CO stretching frequency allowed us to approximate surface coverages. The linewidths of the on-top and hollow peak at ~0.7 ML (14 and 12 cm^{-1}) and of the bridge peak at 0.6 ML (21 cm^{-1}) were similar to those reported from IRAS (on-top 9 cm^{-1}; hollow 17 cm^{-1}; bridge 14 cm^{-1}) [23].

However, under these conditions the bridge/on-top to hollow/on-top transition was not always complete, e.g. in the 10^{-6} mbar/95 K spectrum in Fig. 1 a broad peak in the bridging region (~1940 cm^{-1}) was still present. We have noticed that the adsorbate structure could be influenced by the way CO was introduced. When the clean Pd(1 1 1) surface was exposed to 10^{-6} mbar CO at 95 K the hollow/on-top CO saturation structure was often not perfectly established, e.g. the hollow peak was absent or the on-top peak was broadened (such as in Fig. 2, dotted line). It appeared that the reduced CO mobility at low temperature produced less-ordered structures while better ordered structures were obtained when the Pd(1 1 1) surface was cooled from 700 to 95 K in 10^{-6} mbar CO (Fig. 2, full line, see also [24,25]). This may be important for high pressure studies since the combined effect of a high CO impingement rate and a reduced CO mobility at low temperature could lead to less ordered non-equilibrium adsorption configurations.

Before high pressure experiments were carried out on the model surfaces several precautions had to be considered. Most important was the gas cleanliness since impurities in the 10^{-4}% range (present in "high purity 4.7 CO") that can be neglected under UHV become relevant at elevated pressure. Fig. 3a, trace (1) shows a mass spectrum taken from 1 mbar CO filled into the gas handling system without cleaning. Gas sampling was made using a quartz capillary inlet connected to a differentially pumped mass spectrometer. Ni-carbonyls

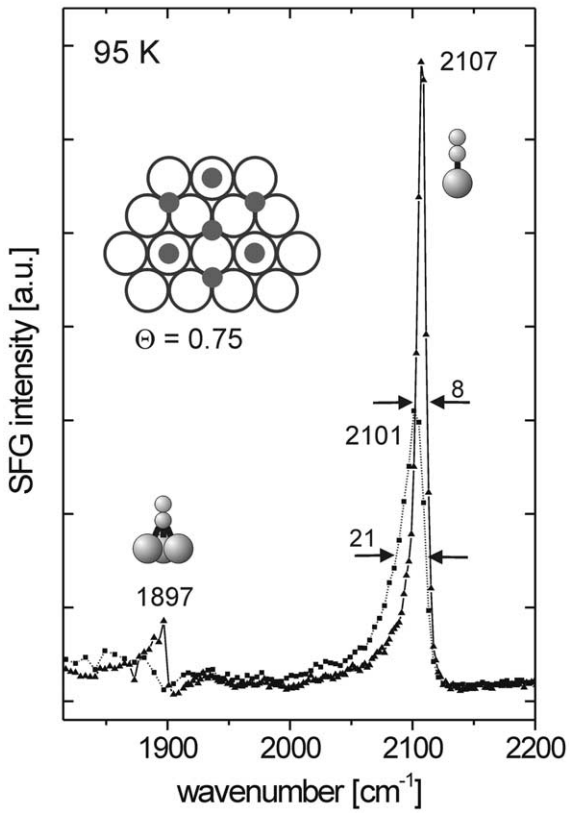

Fig. 2. Effect of annealing on the CO adsorbate structure: SFG spectrum after direct exposure of 10^{-6} mbar CO at 95 K (dotted line) and after annealing in 10^{-6} mbar CO to 700 K with subsequent cooling to 95 K (full line).

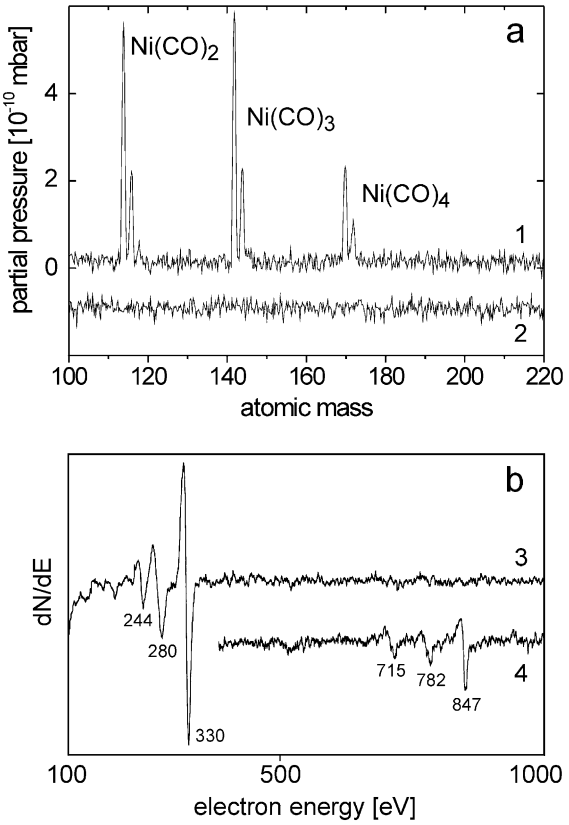

Fig. 3. (a) Mass spectra taken from 1 mbar 4.7 CO using a quartz capillary inlet to a differentially pumped mass spectrometer (1) and after passing CO over a carbonyl absorber cartridge and a cold trap (2). (b) Auger spectra of Pd(1 1 1) (3) and after exposure to 4.7 CO (>200 mbar) for several hours (4) revealing Ni contamination.

can be easily identified that would decompose on the sample leaving behind dispersed Ni. Fig. 3b presents Auger spectra of a clean Pd(1 1 1) surface (trace (3)) and after exposure to 4.7 CO gas (>200 mbar) for several hours (Fig. 3b, trace (4)). Characteristic Ni signatures can be identified at 715, 782 and 847 eV, the attenuation of the Pd signal depends on the amount of Ni. Apparently, Ni contamination can be easily detected but only if the Auger scan is carried out up to ≈900 eV (i.e. not stopped at 600 eV after the oxygen region). If CO adsorbs on the Ni contamination, peak frequencies of 2020–2070 cm^{-1} may occur (depending on the CO coverage [29]) and may be misinterpreted as "high pressure species". Fe-carbonyls may represent a similar problem. In our experiments, the impurities were removed (Fig. 3a, trace (2)), by passing CO over a carbonyl absorber cartridge and a cold trap filled with a liquid nitrogen/ethanol mixture (≈170 K). Water traces at high pressure constitute another problem, in particular, when long time experiments are carried out below the desorption temperature of water (∼160 K for Pt and ∼175 K for Pd). In a previous paper on CO/Pt(1 1 1) [30] we have stressed that great care has to be taken to control the CO cleanliness during high pressure experiments. For CO/Pt(1 1 1) we have observed that coadsorbed water induced a 15 cm^{-1} redshift of the on-top CO frequency that could also be wrongfully inter-

preted as high pressure species. The high pressure experiments described below were therefore carried out at 190 K or above. This should also provide a CO mobility that is high enough to avoid non-equilibrium structures.

There is another effect that must be accounted for in high pressure SFG experiments. Eq. (1) indicates that the SFG intensity depends on the IR and vis intensities. Although no SFG signal is generated by gas phase CO, the SFG process is indirectly influenced by the gas environment since above 1 mbar CO a significant part of the IR light is absorbed in the gas phase. The IR energy arriving at the sample surface and the generated SFG signal thus depend on the gas pressure. In our setup the distance between the input window and the sample is only 1.5 cm, for experimental arrangements using longer beam paths the absorption is even more pronounced. To compensate this effect the reflected IR energy was measured during the experiment, recalculated to the sample position (accounting for the additional absorption between the sample position and the IR detector) and used to normalize the SFG signal. Simultaneously, the vis intensity was recorded with a photodiode. The SFG spectra were then normalized by dividing the experimental plots by the corresponding gas phase absorption curves. Because the IR energy was too small to be directly monitored during the experiments on Pd nanoparticles, SFG spectra of a GaAs reference placed at the sample position inside the high pressure cell were acquired at varying CO pressure and used to normalize for IR absorption (see Fig. 1 in Ref. [30]). To exclude the attenuation of the IR beam by atmospheric CO_2 and water most of the beam path was encapsulated and purged with dry nitrogen.

After considering the precautions raised above, high pressure experiments were carried out at 190 K. While at 95 K ~10–20 Langmuirs CO were sufficient to produce saturation (0.75 ML) on Pd(1 1 1), at 190 K saturation cannot be obtained under UHV, but only when the pressure was significantly increased. This is illustrated in Fig. 4. The first measurement was taken from the clean surface without CO and shows the (invariant) nonresonant background. Similar to the exposure series in Fig. 1, CO adsorbed in bridge and on-top sites which progressively turned into a combination of hollow and on-top. First CO resonances could be observed at 10^{-6} mbar at 1955 cm^{-1} and 2087 cm^{-1} (Fig. 4a). The on-top peak was found to increase with coverage, whereas the intensity of the bridge bonded signal decreased. At 10^{-6} and 10^{-4} mbar two on-top species could be distinguished. Beside the 2087 cm^{-1} resonance there was a peak

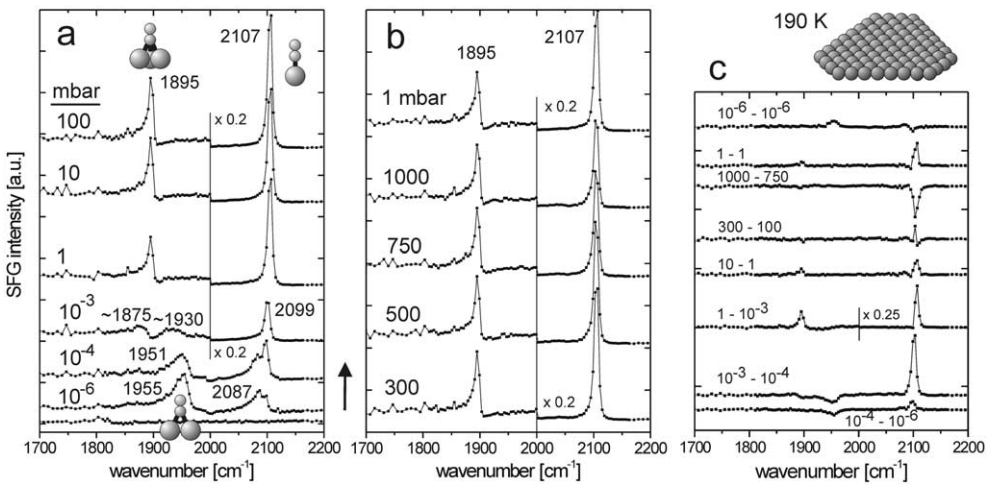

Fig. 4. SFG spectra of CO adsorption on Pd(1 1 1) at 190 K from 10^{-6} to 100 mbar (a) and from 300 to 1000 mbar (b). The final spectrum at 1 mbar demonstrates the reversibility of the adsorbate structure. Difference spectra are displayed in (c).

at 2099 cm^{-1} which finally shifted to 2107 cm^{-1}. It is possible that the 2087 cm^{-1} peak originates from CO linearly bound to steps or defects and that the 2099 cm^{-1} peak is due to on-top CO on the (1 1 1) terraces. Alternatively, the presence of CO domains with different coverage (and hence different CO coupling) may be responsible. Transition from bridge/on-top (0.63 ML) to hollow/on-top (0.75 ML) occupancy occurred above 10^{-3} mbar. The 0.75 ML coverage was fully attained with a CO pressure of 1 mbar at 190 K. The spectral changes can be more clearly followed by the difference spectra in Fig. 4c. Further increase in pressure up to 300 mbar lead to an enhancement of the CO on-top resonance (Fig. 4b and c). It should be noted that without the proper IR absorption correction the raw data would indicate a decrease of on-top CO (due to the decreasing IR energy), an effect that has been misinterpreted in the past [30,45]. For pressures higher than 500 mbar, no more frequency shifts were observed but the on-top signal was reduced (Fig. 4c). The decrease of the on-top signal is probably related to some uncertainty in the IR normalization and doesn't reflect a real disappearance of on-top CO for the following reasons: the on-top peak which is located at an IR absorption maximum (see Ref. [30]) decreased without a frequency shift while the hollow peak which is outside the IR absorption range remained constant. At the highest pressures about 70% to 90% of the IR light is absorbed in the gas phase leading to smaller (noisier) IR and SFG signals which make a quantitative analysis difficult. The 1 mbar and 10^{-6} mbar spectra were recorded once more at the end of the high pressure measurement and the previous spectra could be reproduced with only minor differences in intensity (Fig. 4b and c). This indicates that no pronounced irreversible surface transformations or contamination were present under high pressure conditions.

The spectrum at 10 mbar CO/190 K in Fig. 4 agrees well with the corresponding IRAS spectrum reported by Kuhn, Szanyi and Goodman [24] (except from peak intensities). Goodman and coworkers have removed the gas phase contribution by subtracting IR gas phase spectra (measured on the clean Pd(1 1 1) surface around 1000 K) from the sample spectra. This allowed them to monitor the bridge/on-top to hollow/on-top transition up to 10 mbar and up to 1000 K. At 190 K, a transition at 10^{-3} mbar was suggested, which is identical with our experimental result. Although Goodman and coworkers did not take spectra above 10 mbar CO, they have constructed a "phase diagram" and predicted transition pressures for higher temperatures, e.g. around 650 mbar CO for 300 K. Indeed, when SFG spectra were taken at 300 K, more than 700 mbar CO were necessary to reach saturation, in fair agreement with the prediction by Goodman and coworkers [24,40]. At 400 K, the corresponding coverages were even smaller and at 1 bar pressure a coverage of about 0.6 ML was observed.

A comparison of Figs. 1 and 4 shows that the high pressure adsorbate structures of CO (up to 1000 mbar) were very similar to the high coverage structures observed under UHV by SFG or IRAS. There is no evidence for the formation of high pressure species that are different from those observed under UHV. Small differences may occur at low temperatures (around 100 K) when less-ordered layers may be formed (Fig. 2). While high CO pressures have been reported to disrupt Rh nanoparticles [5] and restructure Pt single crystals [46], under our experimental conditions such an effect was absent for Pd(1 1 1). No evidence for major surface rearrangements has been found. The spectra were fully reversible with pressure even after several hours of gas exposure.

Since we were aiming at studying Pd nanoparticles, a less ordered surface may be a better reference. SFG was therefore also performed on defect-rich Pd(1 1 1) (Fig. 5). As described in Section 2, this surface can be imagined as being composed of (1 1 1) terraces and various sorts of "defects" including steps and kinks. Comparison of the 10^{-6} mbar CO spectrum to the corresponding spectrum of the well-ordered (1 1 1) surface (Fig. 4) shows an additional peak on the imperfect surface at 1980 to 1990 cm^{-1}. We suggest that this species is related to CO adsorbed on step (low coordination) sites and the frequency range indicates that it is bridge bonded CO. This species could also be observed on a strongly sputtered (1 1 1) surface. Bridge bonded species around 1985 cm^{-1} have previously been assigned to CO

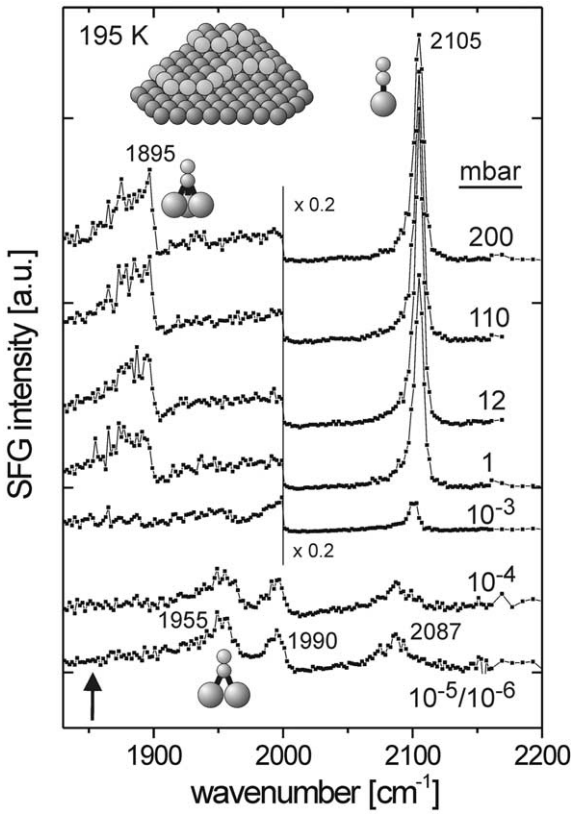

Fig. 5. SFG spectra of CO adsorption on defect-rich Pd(1 1 1) at 195 K from 10^{-6} to 200 mbar. Compared to the perfect (1 1 1) surface an additional peak at 1990 cm^{-1} appeared.

on Pd(1 0 0) [23,40,47], Pd(1 1 0) [28,48], Pd(2 1 0) [23] and rough Pd thin films [23]. This vibrational mode should also occur when CO is adsorbed on curved and rough surfaces of nanoparticles. It has indeed been observed by infrared spectroscopy on Pd particles on silica prepared by impregnation [27,49], and on alumina [26,50] and titania [28] supported Pd model catalysts.

The species at 1980 to 1990 cm^{-1} may originate from a specific binding site at a step edge but it may also arise from coupling between CO molecules on a step and neighboring CO molecules on a (1 1 1) terrace. Greenler and coworkers [51] have demonstrated that by dipole coupling of linear CO molecules on a step edge (where the metal atoms have coordination numbers < 9) and (''subsequent'') coupling to CO adsorbed on the terrace sites (coordination number $= 9$) a resonance frequency is produced that is characteristic rather for the ensemble and not so much for a particular binding site. In any case, the ''normal'' bridge peak at 1930 to 1950 cm^{-1} and the on-top peak show a behavior very similar as on smooth Pd-(1 1 1). When the pressure was increased on the imperfect Pd(1 1 1) crystal at 190 K (Fig. 5) the bridge/on-top to hollow/on-top transition again occurred around 10^{-3} to 1 mbar, i.e. nearly identical to Pd(1 1 1). Although the hollow peak was very noisy the transition itself seemed not to be heavily influenced by the presence of defects.

3.2. Adsorption of CO on Pd/Al_2O_3

We will now compare the results on Pd(1 1 1) and ''rough'' Pd(1 1 1) to SFG spectra of CO adsorbed on alumina supported Pd nanoparticles. A detailed description of the cluster SFG spectra has been presented elsewhere [20]. Only one example is shown here and contrasted to Pd(1 1 1). The linewidths of the nanoparticle spectra were broader than those of single crystal spectra for two reasons. First, the heterogeneity of supported nanoparticles with respect to particle size and surface structure generally leads to broader peaks (for instance about 20-25 cm^{-1} in IRAS [50]) and, second, the OPG/DFG unit utilized in the cluster experiments had a lower resolution ($\sim$25 cm^{-1}). The convolution of both effects resulted in peaks of about 35 cm^{-1} FWHM.

Fig. 6a shows SFG spectra of CO on Pd particles of 6 nm mean size (about 4000 atoms/particle) taken at 190 K between 10^{-7} and 200 mbar CO background pressure. The Pd particles were grown at 300 K and exhibited the shape of a truncated cuboctahedron with mainly (1 1 1) and (1 0 0) surface facets, as shown by atomically resolved STM (scanning tunneling microscopy) images by Hansen et al. [52]. A ball model and an STM image are shown in Fig. 6b and c (high resolution STM images are found in Refs. [32,52,53]). The (1 1 1) top facet dominates the particle morphology with smaller contributions of (1 1 1) and (1 0 0) side facets. CO adsorbed on the side facets is tilted with respect to the underlying metal substrate and should produce only a small signal (according to

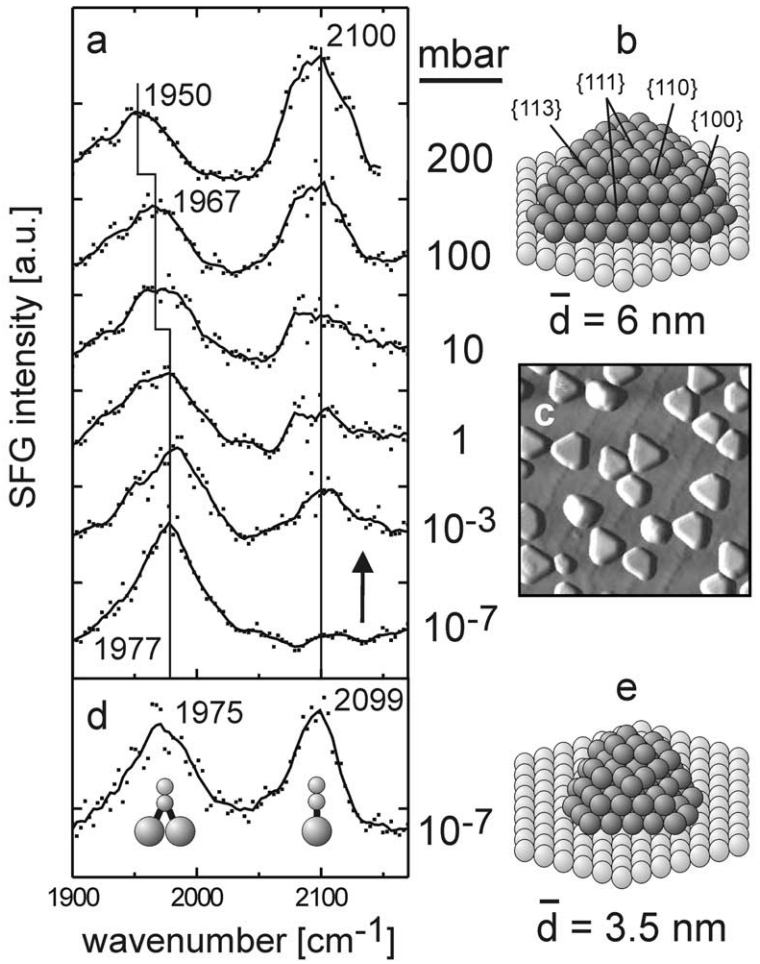

Fig. 6. SFG spectra of CO adsorption on Al_2O_3 supported Pd nanoparticles between 10^{-7} and 200 mbar CO and at 190 K. Spectra (a) were taken from well-faceted Pd particles with a mean size of 6 nm. A model and an STM image (CCT, 50 × 50 nm, image adapted from Ref. [53]) are displayed in (b,c). The 10^{-7} mbar spectrum of 3.5 nm Pd particles exhibiting rough surfaces and the corresponding model are presented in (d,e).

the IR surface selection rule [23]). Accordingly, the 6 nm particles should behave similar to a (1 1 1) surface.

Coming back to the SFG spectra, two parameters should be considered when comparing nanoparticles and Pd(1 1 1): the resonance frequencies and the relative ratio of on-top/bridge adsorption. At 10^{-7} mbar CO a pronounced band was observed at 1977 cm^{-1} and assigned to bridge bonded CO, whereas the on-top CO signal was much smaller (Fig. 6a), in agreement with previous IRAS data [50]. It was mentioned before that a quantitative analysis is difficult but if we take the integrated SFG signal intensity as a rough estimate the on-top/bridge ratio is ~0.2 on Pd(1 1 1) and <0.1 on the nanoparticles. However, the resonance frequency of 1977 cm^{-1} is different from the Pd(1 1 1) value of 1955 cm^{-1}. In light of SFG spectra obtained from defect-rich Pd(1 1 1) we suggest the peak at 1977 cm^{-1} to be related to CO adsorption on surface steps and/or particle edges. As shown by HR-TEM [6] monoatomic steps are even present on well-faceted nanoparticles, since a cuboctahedron with complete surfaces would re-

quire a "magic number" of atoms for a given size. Consequently, some surface steps (or {1 1 0} and {1 1 3} nanofacets) were included in the ball model in Fig. 6b. It is therefore not surprising that the resonance frequency of bridge bonded CO is different on nanoparticles and on Pd(1 1 1). IRAS spectra of $CO/Pd/Al_2O_3/NiAl(1\,1\,0)$ had shown a third weaker band around 1950 cm^{-1} that was assigned to CO bridge bonded on (1 1 1) terraces. It was not possible to detect the weaker species with SFG since the defect-related species dominated. Similar IR spectra were also reported for $Pd/Al_2O_3/Ta(1\,1\,0)$ model catalysts [26] and for impregnated Pd/SiO_2 [27].

When the CO pressure was increased the bridge bonded CO peak decreased in intensity and shifted to lower wavenumber while the on-top peak increased (Fig. 6a; on-top/bridge ratio 10^{-3} mbar: 0.5; 1 mbar: 0.5; 10 mbar: 0.7; 100 mbar: 1.2; 200 mbar: 1.7). Similar spectral changes on Pd(1 1 1) occurred in Figs. 4 and 5 during the bridge/on-top to hollow/on-top transition. However, while bridge bonded CO disappeared on Pd(1 1 1) around 1 mbar, this species persisted even up to 200 mbar on the Pd aggregates. As already mentioned earlier, the hollow site region could not be properly investigated because of the severe drop of the IR power for frequencies below 1900 cm^{-1}. Gelin and Yates [27] and Rainer et al. [26] report a similar behavior for Pd particles on silica and alumina. This effect may be related to the heterogeneity of the particle surface that prevents the lateral CO interactions steering the phase transition to (fully) establish.

Similar measurements were also carried out on even "rougher" Pd particles with a mean diameter of 3.5 nm (about 850 atoms/particle) (Fig. 6d and e). These particles were grown at 90 K and the reduced Pd mobility leads to a higher nucleation density (4.5×10^{12} cm^{-2}), to a smaller particle size, and also to less ordered surfaces with more low-coordination sites (surface defects, edges, steps, etc.). Considering the 10^{-7} mbar/190 K SFG spectrum in Fig. 6d, it should be noticed that two peaks were observed and assigned to bridge bonded CO (the frequency of 1975 cm^{-1} again pointing to a defect-related bridge species) and to on-top CO (2099 cm^{-1}). In contrast to the corresponding spectrum of 6 nm particles (Fig. 6a) the fraction of adsorbed on-top CO is much higher (on-top/bridge ratio of ~0.8). This indicates that smaller Pd aggregates possess a highly defective structure and corroborates IRAS data of Pd particles and rough Pd thin films [23,50].

With increasing pressure only minor changes were observed (spectra not shown). The signal of bridge bonded CO decreased slightly in intensity and shifted to lower frequencies (on-top/bridge ratio 10^{-7} mbar: 0.8; 10^{-3} mbar: 1.2; 1 mbar: 1.5; 10 mbar: 1.6; 100 mbar: 1.7; 200 mbar: 1.9). At 200 mbar CO, a spectrum basically identical to the 200 mbar spectrum of the 6 nm particles was obtained. Again, the transition to the hollow/on-top configuration was only partially manifesting itself whereas on Pd(1 1 1) the same transition occurred at much lower CO pressure (~1 mbar; c.f. Fig. 4). The defect concentration on defect-rich Pd(1 1 1) was apparently too low to prevent the adsorbate rearrangement (cf. Fig. 5).

When spectra were taken at 300 K only a small on-top peak could be observed at 10^{-7} mbar even on the 3.5 nm Pd particles [20]. This can be understood on the basis of TPD results indicating that on-top CO desorbs around 250 K. With increasing pressure the on-top peak became more intense but its intensity never exceeded the bridge peak. To obtain an adsorption site occupancy similar to the 10^{-7} mbar/190 K spectrum in Fig. 6d, a pressure of about 200 mbar was necessary at 300 K. Finally it should be mentioned that the 10^{-7} mbar particle spectra could be reproduced after the high gas pressure was pumped out and no indications for CO-induced particle disrupture were observed.

One of the main objectives of SFG is to carry out spectroscopy during catalytic reactions. However, this will provide meaningful results only if the model catalyst under investigation closely mimics the properties of a conventional (impregnated) catalyst. As a first step in this direction, we have utilized ethylene hydrogenation at a total pressure of 1 bar to determine the activity of $Pd/Al_2O_3/NiAl(1\,1\,0)$ model catalysts. The SFG cell was employed as recirculated batch reactor and interfaced to a gas chromatograph for product analysis. The (background activity) of $Al_2O_3/NiAl(1\,1\,0)$ was negligible with only 0.2% of the Pd activity.

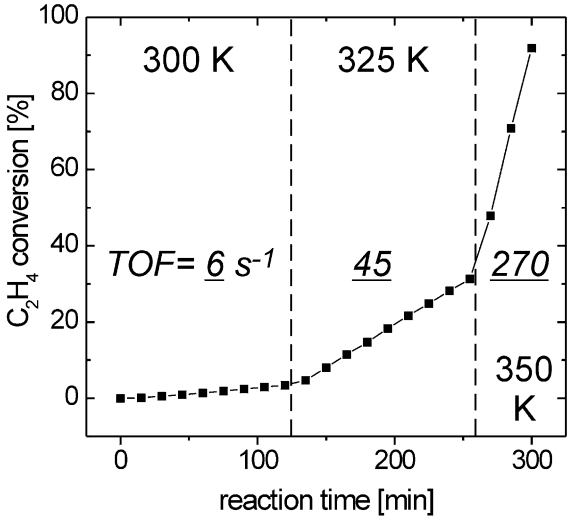

Fig. 7. Ethylene hydrogenation activity of a $Pd/Al_2O_3/NiAl(1\,1\,0)$ model catalyst with a mean Pd particle size of 3.5 nm. The reaction was carried out with 50 mbar C_2H_4, 215 mbar H_2 and 770 mbar He at 300 to 350 K. Because the SFG cell was used as a recirculated batch reactor, the conversion increased with time. Turnover frequencies for the different temperatures are also indicated.

Fig. 7 shows results for 3.5 nm Pd particles exposed to 50 mbar ethylene, 215 mbar hydrogen and 770 mbar helium. The ethylene conversion (% consumed) is plotted versus time for three temperatures (300, 325 and 350 K). At each temperature the turnover frequency (TOF; molecules ethane produced per Pd surface atom and second) was quite constant (e.g. over 3 h at 300 K) and "steady state" values are indicated. With increasing temperature 50 mbar C_2H_4 could be converted within 5 hours. The turnover frequencies, reaction orders (ethylene: −0.3; hydrogen: 1; not shown) and the activation energy (about 50–60 kJ/mol) were very similar to values reported for impregnated powder catalysts [54,55]. Further experiments including various particle sizes and SFG spectroscopy are in progress but the preliminary results already indicate that our model is well suited for catalytic tests at ambient pressure.

4. Conclusions

We have applied non-linear optical SFG vibrational spectroscopy to study the adsorption of CO on various Pd model catalysts, ranging from ideal Pd(1 1 1) surfaces over defect-rich Pd(1 1 1) to well faceted and rougher Pd nanoparticles. The spectral resolution of SFG is comparable to IRAS, while a quantitative analysis of SFG spectra is still difficult. However, SFG spectroscopy is not restricted to a low pressure environment and the combination of a surface analysis chamber with an SFG-compatible UHV-high pressure cell allows to study adsorbates on well-defined surfaces from submonolayer coverages up to ambient gas pressure.

Under the conditions studied we did not find evidence for the formation of high pressure species that are different from those observed under UHV. The high pressure adsorbate structures of CO (up to 1000 mbar) were very similar to the high coverage structures observed under UHV. Small differences may occur at low temperature (around 100 K) when less-ordered (non-equilibrium) structures were formed. Our spectra were fully reversible with pressure and no evidence for major surface rearrangements has been found.

At low pressure (10^{-7} mbar) the CO adsorption site occupancy was mainly governed by the surface structure of the different model surfaces. Each surface showed a characteristic spectrum, i.e. with specific resonance frequencies and hollow/bridge/on-top ratios. It is clear that e.g. a Pd(1 1 1) surface can hardly model the situation encountered on Pd nanoparticles. Even on well-faceted Pd particles the bridged CO frequency was different from Pd(1 1 1) and more similar to stepped Pd(1 1 1). In addition, the evolution of the CO spectra with increasing pressure depended also on the Pd morphology. On Pd(1 1 1) a rearrangement of the CO layer from a bridge/on-top to a hollow/on-top configuration occurred at 1 mbar at 190 K while the curved surface of Pd particles prevented this transition even though a much higher pressure was applied (200 mbar). Apparently, the saturation structure on Pd(1 1 1) only plays a minor role on Pd particles, again demonstrating the different behavior of the two surfaces.

When high pressure experiments are carried out, great care has to be taken to control impurities that can be generally neglected under UHV conditions. Without thorough gas cleaning Ni-carbonyls can be deposited on the sample leading to

additional peaks around 2050 cm^{-1} that may be misinterpreted as high pressure species. Water traces in the high pressure gas constitute another problem, in particular, when long time experiments are carried out below the desorption temperature of water. Coadsorbed water may induce a frequency shift that could also be wrongfully interpreted as high pressure effect.

Apparently, there is a "materials gap", i.e. the properties of nanoparticles cannot be fully modeled by extended single crystal surfaces and vice versa. The "pressure gap" may be more a "coverage gap". We have observed the same adsorbate species under UHV and high pressure, but one should keep in mind that at elevated temperature coverages obtainable under UHV may not be in a range relevant for a specific reaction.

Acknowledgements

Part of this work was supported by the Priority Program SPP 1091 of the German Science Foundation (DFG). H.U. is grateful for a DFG fellowship. We also thank M. Heemeier and M. Bäumer (FHI Berlin) for allowing to use their STM data (Fig. 6c).

References

[1] J.M. Thomas, G.A. Somorjai (Eds.), Topics in Catalysis, Special Issue on in-situ Characterization of Catalysts, vol. 8, 1999.
[2] R. Schlögl, A. Zecchina (Eds.), Topics in Catalysis, Special Issue on in-situ Characterization of Catalysts, vol. 15, 2001.
[3] J.A. Jensen, K.B. Rider, M. Salmeron, G.A. Somorjai, Phys. Rev. Lett. 80 (1998) 1228.
[4] G.A. Somorjai, G. Rupprechter, J. Phys. Chem. B 103 (1999) 1623.
[5] A. Berkó, G. Ménesi, F. Solymosi, J. Phys. Chem. 100 (1996) 17732.
[6] G. Rupprechter, H.-J. Freund, Top. Catal. 14 (2001) 3.
[7] A. Eppler, G. Rupprechter, E.A. Anderson, G.A. Somorjai, J. Phys. Chem. B 104 (2000) 7286.
[8] G. Rupprechter, K. Hayek, H. Hofmeister, J. Catal. 173 (1998) 409.
[9] C. Stampfl, M. Scheffler, Surf. Sci. 433–435 (1999) 119.
[10] A. Knop-Gericke, M. Hävecker, T. Schedel-Niedrig, R. Schlögl, Top. Catal. 15 (2001) 27.
[11] Y.R. Shen, Surf. Sci. 299/300 (1994) 551.
[12] R.B. Hall, J.N. Russell, J. Miragliotta, P.R. Rabinowitz, in: R. Vanselow, R. Howe (Eds.), Chemistry and Physics of Solid Surfaces (Springer Series in Surface Science), vol. 22, Springer, Berlin, 1990, p. 87.
[13] G.L. Richmond, Annu. Rev. Phys. Chem. 52 (2001) 357.
[14] K.B. Eisenthal, Chem. Rev. 96 (1996) 1343.
[15] C. Klünker, M. Balden, S. Lehwald, W. Daum, Surf. Sci. 360 (1996) 104.
[16] X. Su, P.S. Cremer, Y.R. Shen, G.A. Somorjai, J. Am. Chem. Soc. 119 (1997) 3994.
[17] H. Härle, K. Mendel, U. Metka, H.R. Volpp, L. Willms, J. Wolfrum, Chem. Phys. Lett. 279 (1997) 275.
[18] A. Bandara, S. Dobashi, J. Kubota, K. Onda, A. Wada, K. Domen, C. Hirose, S. Kano, Surf. Sci. 387 (1997) 312.
[19] H. Härle, U. Metka, H.-R. Volpp, J. Wolfrum, Phys. Chem. Chem. Phys. 1 (1999) 5059.
[20] T. Dellwig, G. Rupprechter, H. Unterhalt, H.-J. Freund, Phys. Rev. Lett. 85 (2000) 776.
[21] S. Baldelli, A.S. Eppler, E. Anderson, Y.R. Shen, G.A. Somorjai, J. Chem. Phys. 113 (2000) 5432.
[22] M. Tüshaus, W. Berndt, H. Conrad, A.M. Bradshaw, B. Persson, Appl. Phys. A 51 (1990) 91.
[23] F.M. Hoffmann, Surf. Sci. Rep. 3 (1983) 103.
[24] W.K. Kuhn, J. Szanyi, D.W. Goodman, Surf. Sci. Lett. 274 (1992) L611.
[25] B. Bourguignon, S. Carrez, B. Dragnea, H. Dubost, Surf. Sci. 418 (1998) 171.
[26] D.R. Rainer, M.-C. Wu, D.I. Mahon, D.W. Goodman, J. Vac. Sci. Technol. A 14 (1996) 1184.
[27] P. Gelin, A. Siedle, J. Yates, J. Phys. Chem. 88 (1984) 2978.
[28] J. Evans, B.E. Hayden, G. Lu, Surf. Sci. 360 (1996) 61.
[29] G. Rupprechter, T. Dellwig, H. Unterhalt, H.-J. Freund, Top. Catal. 15 (2001) 19.
[30] G. Rupprechter, T. Dellwig, H. Unterhalt, H.-J. Freund, J. Phys. Chem. B 105 (2001) 3797.
[31] H. Unterhalt, M. Morkel, P. Galletto, G. Rupprechter, H.-J. Freund, to be submitted (2002).
[32] M. Bäumer, H.-J. Freund, Prog. Surf. Sci. 61 (1999) 127.
[33] A. Tadjeddine, A. Le Rille, O. Pluchery, F. Vidal, W.Q. Zheng, A. Peremans, Phys. Stat. Sol. (a) 175 (1999) 89.
[34] Y. Caudano, A. Peremans, P.A. Thiry, P. Dumas, A. Tadjeddine, Surf. Sci. 368 (1996) 337.
[35] R. Braun, B.D. Casson, C.D. Bain, E.W.M. van der Ham, Q.H.F. Vrehen, E.R. Eliel, A.M. Briggs, P.B. Davies, J. Chem. Phys. 110 (1999) 4634–4640.
[36] S. Lin, A. Oldfield, D. Klenerman, Surf. Sci. 464 (2000) 1.
[37] X.D. Zhu, H. Suhr, Y.R. Shen, Phys. Rev. B 35 (1987) 3047.
[38] H. Conrad, G. Ertl, J. Küppers, Surf. Sci. 76 (1978) 323.
[39] H. Ohtani, M.A. Van Hove, G.A. Somorjai, Surf. Sci. 187 (1987) 372.
[40] J. Szanyi, W.K. Kuhn, D.W. Goodman, J. Vac. Sci. Technol. A 11 (1993) 1969–1974.
[41] S. Surnev, M. Sock, M.G. Ramsey, F.P. Netzer, M. Wiklund, M. Borg, J.N. Andersen, Surf. Sci. 470 (2000) 171.

[42] T. Gießel, O. Schaff, C.J. Hirschmugl, V. Fernandez, K.M. Schindler, A. Theobald, S. Bao, R. Lindsay, W. Berndt, A.M. Bradshaw, C. Baddeley, A.F. Lee, R.M. Lambert, D.P. Woodruff, Surf. Sci. 406 (1998) 90.
[43] D. Loffreda, D. Simon, P. Sautet, Surf. Sci. 425 (1999) 68.
[44] S. Baldelli, N. Markovic, P. Ross, Y.R. Shen, G.A. Somorjai, J. Phys. Chem. B 103 (1999) 8920.
[45] K.Y. Kung, P. Chen, F. Wei, Y.R. Shen, G.A. Somorjai, Surf. Sci. Lett. 463 (2000) L627.
[46] B.J. McIntyre, M. Salmeron, G.A. Somorjai, J. Vac. Sci. Technol. A 11 (1993) 1964.
[47] R.J. Behm, K. Christmann, G. Ertl, J. Chem. Phys. 73 (1980) 2984.
[48] R. Raval, S. Haq, M.A. Harrison, G. Blyholder, D.A. King, Chem. Phys. Lett. 167 (1990) 391.
[49] G.C. Cabilla, A.L. Bonivardi, M.A. Baltanas, Catal. Lett. 55 (1998) 147.
[50] K. Wolter, O. Seiferth, H. Kuhlenbeck, M. Bäumer, H.-J. Freund, Surf. Sci. 399 (1998) 190.
[51] R.K. Brandt, M.R. Hughes, L.P. Bourget, K. Truszkowska, R.G. Greenler, Surf. Sci. 286 (1993) 15.
[52] K.H. Hansen, T. Worren, S. Stempel, E. Lægsgaard, M. Bäumer, H.-J. Freund, F. Besenbacher, I. Stensgaard, Phys. Rev. Lett. 83 (1999) 4120.
[53] Sh. Shaikhutdinov, M. Heemeier, M. Bäumer, T. Lear, D. Lennon, R.J. Oldman, S.D. Jackson, H.-J. Freund, J. Catal. 200 (2001) 330.
[54] T. Beebe, J.T. Yates, J. Am. Chem. Soc. 108 (1986) 663.
[55] R.J. Davis, M. Boudart, Catal. Sci. Technol. 1 (1991) 129.